Optical Fiber Technology 31 (2016) 83–91

Contents lists available at ScienceDirect

Optical Fiber Technology

www.elsevier.com/locate/yofte

Regular Articles

Numerical analysis of residual stresses in preforms of stress applying part for PANDA-type polarization maintaining optical fibers in view of technological imperfections of the doped zone geometry

Aleksandr N. Trufanov *, Nikolay A. Trufanov, Nikita V. Semenov

Department of Computational Mathematics and Mechanics, Perm National Research Polytechnic University, 29 Komsomolsky Ave, Perm 614990, Russia

A R T I C L E   I N F O

Article history:
Received 23 September 2015
Revised 1 February 2016
Accepted 11 June 2016

Keywords:
Finite element method
Polarization maintaining fiber
Vitrification
Residual stresses
Relaxation transition

A B S T R A C T

The experimental data analysis of the stress applying rod section geometry for the PANDA-type polarization maintaining optical fiber has been performed. The dependencies of the change in the radial dimensions of the preform and the doping boundary on the angular coordinate have been obtained. The original algorithm of experimental data statistic analysis, which enables determination of the specimens' characteristic form of section, has been described. The influence of actual doped zone geometry on the residual stress fields formed during the stress rod preform fabrication has been investigated. It has been established that the deviation of the boundary between pure silica and the doped zone from the circular shape results in dissymmetry and local concentrations of the residual stress fields along the section, which can cause preforms destruction at high degrees of doping. The observed geometry deviations of up to 10% lead to the increase of the maximum stress intensity value by over 20%.

1. Introduction

Polarization maintaining quartz optical fibers that maintain signal polarization due to specially formed residual stress fields in the light-guiding core are widely used for the manufacture of fiber-optic sensors [1,2]. The necessary stress–strain state in the PANDA-type optical fiber is created by the introduction into the fiber drawing preform of the stress elements from doped silica glass with a much higher linear thermal expansion coefficient than in other materials of the structure. Such fibers have two round cylindrical stress rods with a variable content of dopants along the radius, which are fabricated by the modified chemical gas phase deposition (MCVD) [3], at which particles of doped fused silica are deposited on the internal surface of the silica glass tube at high temperature and then the tube collapses and cools. Such rods are installed into the ready openings in the preform which is then softened under high temperature and drawn into fiber. After drawing and cooling the fiber develops inner stresses. The stress state of the anisotropic optical waveguide is defined by a combination of factors connected with the material properties and manufacturing process conditions: inhomogeneity of temperature fields, thermal strain incompatibility of the inhomogeniously doped elements, and thermal relaxation transitions (vitrification-softening) due to non-uniform doping under different temperature ranges. The introduction of stress rods into the fiber structure results in the inhomogeneous stress field in the cross-section of the light-guiding core. The higher principal stress difference in the core is, the higher the mode birefringence value is [4], a key characteristic of the PM optical fiber.

When modeling the PANDA-type fiber, it is usually assumed that stress rods have axial symmetry and, accordingly, their sections are circular in shape [5–7], but in practice, the section geometry depends on many factors determined by the manufacturing process and, as a rule, geometrics of actual products differ from the design values. The section form deviation from the circular shape can affect the strength of rods and the optical characteristics of fibers in which such stress elements are used.

Basing on the measurements, analysis and statistical treatment of geometric parameters of the manufactured batch of stress rods for the PANDA PM fiber preforms the paper establishes regularities which describe possible deviations of the doped zone boundary. The results of numerical experiments based on solving the problem of thermomechanical behavior of the stress rod preform at cooling from 2100 °C to the ambient temperature subject to the relaxation transition from the softened condition to the glassy one are presented. The effect of the doped zone form deviations on the stress–strain state of the stress rod preform is investigated.

* Corresponding author.
E-mail address: ant@pstu.ru (A.N. Trufanov).

http://dx.doi.org/10.1016/j.yofte.2016.06.004
1068-5200/

2. Data acquisition technology

The tested rods geometrics were measured with a Photon Kinetics 2600 preforms analyzer. The device allows the preform rotation by the known angle and selection of the section along the rod. The refractive index profile in the preform section was analyzed and the boundaries between optical media of different density were determined.

The examined stress rods were manufactured on the same equipment, had the same design and consisted of three different in the chemical composition layers (Fig. 1).

For each rod, the Γ_1, Γ_2 and Γ_3 boundaries positions in 15 radial sections (30 points for each boundary) in 10 axial sections were obtained. Fig. 2 shows the data received for a typical cross-section as an example. One hundred rods were investigated altogether, for which 30 radii values for each of 3 boundaries in 10 axial sections were determined:

$$R_{nij}(\varphi_k) n = \overline{1,3}, \quad i = \overline{1,100}, \quad j = \overline{1,10}, \quad k = 1,30,$$

where n is the boundary number, i is the rod number from the set, j is the lengthwise section number, and k is the angular section number.

3. Experimental statistics

The analysis of data at the Γ_1 and Γ_3 boundaries showed that deviations from design values are insignificant (spread of $R_{1ij}(\varphi_k)$ and $R_{3ij}(\varphi_k)$ values is within 3% of average), but at the Γ_2 boundary between the pure silica glass zone and the doped part the $R_{2ij}(\varphi_k)$ values spread proved to be markedly higher, up to 10% from average values. On this ground, the paper investigates the dependence of the boundary Γ_2 deviation from the design shape and the data at Γ_1 and Γ_3 boundaries are not further analyzed.

To simplify notations we take n equal to two and omit $R_{ij}(\varphi_k) = R_{2ij}(\varphi_k)$.

Let us consider the radius function of an angular coordinate $R_{ij}(\varphi_k)$ to be a random variable, where i is the rod number, j is the axial section number and k is the angular coordinate number.

Data analysis has shown that along the axial sections of a single rod the doping zone boundary Γ_2 stays about the same. Therefore, to describe its geometry we can use arithmetic mean of the radii measured for equal values of the angle φ in 10 axial sections:

$$R_i(\varphi_k) = \sum_{j=1}^{10} \frac{R_{ij}(\varphi_k)}{10}. \quad (1)$$

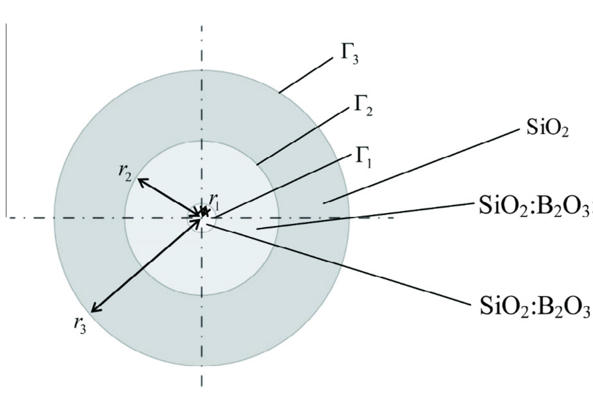

Fig. 1. Axial section S of the stress rod preform: Γ_1 is the boundary between the inner and center doped layers, Γ_2 is the boundary between the center and outer layers, Γ_3 is the outer boundary of the preform.

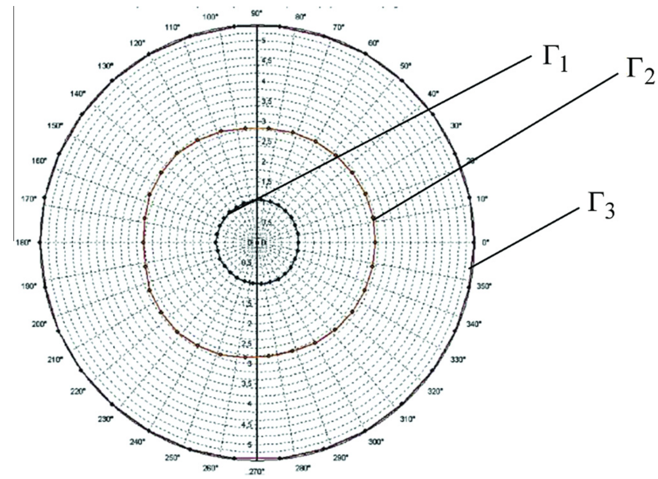

Fig. 2. Dependence of experimentally established radii on the angular coordinate $R_{nij}(\varphi_k)$ for a section of a standard stress rod.

Analysis of $R_i(\varphi_k)$ dependencies for different rods (Fig. 3) enables us to ascertain their qualitative similarity. All diagrams visually show three characteristic 'maximums' and three 'minimums'. In Fig. 3 and further, radii values are written as a ratio of real radius to the mean value across the whole sample.

Since at placing a preform into the analyzer the initial position of the angle reading is not regulated, despite similar geometry, preforms appear to be turned against each other along the angular coordinate. Superposition of diagrams shows no conformity of the general picture without preprocessing, Fig. 4.

To process the measurement results we used the following algorithm:

1. Any dependence from the investigated set $R_n(\varphi_k)$, $n = \overline{1,100}$ is taken as the basis, Fig. 5.
2. A random dependence $R_m(\varphi_k)$, $m \neq n$, $m = \overline{1,100}$ from the investigated set is chosen and checked for correlation with $R_n(\varphi_k)$ by the formula of normalized correlation moment r_{nm}.

$$r_{nm} = \frac{M(R_n - M(R_n))M(R_m - M(R_m))}{\sigma_n \sigma_m}, \quad (2)$$

   where M is mathematical expectation, and σ_n, σ_m are rms deviations for R_n and R_m, respectively.
3. Curves are compared 30 times (the number of points corresponds to the number of possible combinations), with shift occurring every time: all points move to the left and the leftmost one becomes the rightmost $R'_m(\varphi_k) = R_m(\varphi_{k+1})$, $k = \overline{1,29}$ and $R_m(\varphi_{30}) = R_m(\varphi_1)$, Fig. 6.

Among the thirty checked combinations there is one for which the normalized correlation moment with the reference curve n is maximum. The obtained dependence is maximally similar to the reference $R_n(\varphi_k)$ among all possible and holds true in regard to the found left shift of all points by m positions $R'_i(\varphi_k) = R'_m(\varphi_k)$, where $i = m$.

Points 2 and 3 are repeated until data on all studied rods are processed.

The described procedure gives a set of curves $R'_i(\varphi_k)$ (Fig. 7) that correlate among themselves to the maximum (Fig. 8): the normalized correlation moment is $r_{nm} > 0.9$ among all curves.

Thus, deviation of the doped core shape from the circular one is repeated in virtually all articles of the batch. Statistical analysis of